Desalination 468 (2019) 114084

Contents lists available at ScienceDirect

Desalination

journal homepage: www.elsevier.com/locate/desal

Key physicochemical characteristics governing organic micropollutant adsorption and transport in ion-exchange membranes during reverse electrodialysis

M. Roman[a,b,*], L.H. Van Dijk[a], L. Gutierrez[c], M. Vanoppen[b], J.W. Post[a], B.A. Wols[a,d], E.R. Cornelissen[b,d], A.R.D. Verliefde[b]

[a] Wetsus, Centre of Excellence for Sustainable Water Technology, P.O. Box 1113, 8900 CC Leeuwarden, The Netherland
[b] Particle and Interfacial Technology Group, Department of Applied Analytical and Physical Chemistry, Faculty of Bioscience Engineering, Ghent University, Ghent 9000, Belgium
[c] Facultad del Mar y Medio Ambiente, Universidad del Pacifico, Ecuador
[d] KWR Watercycle Research Institute, P.O. Box 1072, 3430 BB Nieuwegein, The Netherlands

GRAPHICAL ABSTRACT

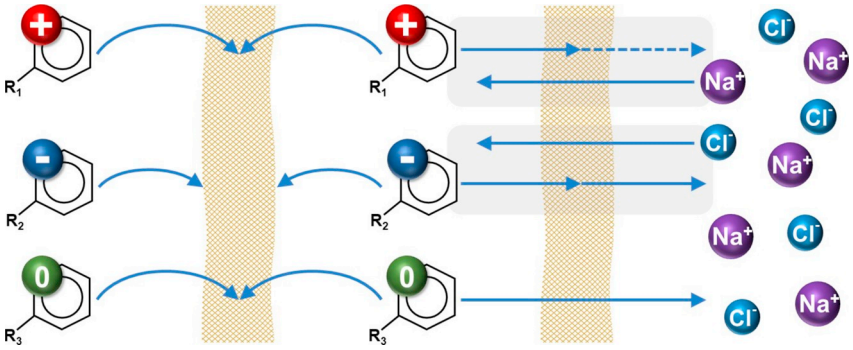

ARTICLE INFO

Keywords:
Organic micropollutants
Seawater desalination
Reverse electrodialysis
Ion-exchange membranes

ABSTRACT

The co-generation of electricity and electrodialysis of seawater in a hybrid system is a promising approach to overcome water scarcity. Reverse electrodialysis harvests energy from the salinity gradient, where seawater is used as a high salinity stream while secondary treated wastewater can be used as a sustainable low salinity stream. Treated wastewater contains organic micropollutants, which can be transported to the seawater stream. The current research establishes a connection between adsorption and transport of organic micropollutants in ion exchange membranes, using a cross-flow stack in adsorption and zero-current experiments. To mimic the composition of treated wastewater, a mixture of nineteen organic micropollutants of varied physicochemical characteristics (e.g. size, charge, polarity, hydrogen donor/acceptor count, hydrophobicity) at environmentally relevant concentrations was used. Depending on the charge, micropollutants develop different types of mechanisms responsible for short-distance interactions with ion-exchange membranes, which has a direct influence in their transport behavior. This study provides a rational basis for the optimization/design of next-generation ion-exchange membranes, in which the permeability toward organic micropollutants should be also included. This investigation highly contributes to understanding the potential hazard posed by organic micropollutants in

* Corresponding author at: Wetsus, Centre of Excellence for Sustainable Water Technology, P.O. Box 1113, 8900 CC Leeuwarden, The Netherland
E-mail address: malgorzata.roman@wetsus.nl (M. Roman).

https://doi.org/10.1016/j.desal.2019.114084
Received 24 May 2019; Received in revised form 16 July 2019; Accepted 16 July 2019
Available online 26 July 2019

reverse electrodialysis in seawater desalination systems, where treated wastewater is used as a low salinity stream.

1. Introduction

The desalination of seawater can provide a steady supply of high-quality drinking water [1–3]. Recent developments in ion-exchange membrane (IEM) technology have allowed electrodialysis (ED) to reach better performances and competitiveness toward other seawater desalination techniques [4]. ED still remains energy and cost intensive in a stand-alone operation mode [5]. Therefore, the co-generation of electricity and ED desalination in a hybrid system is a promising approach for improvement [6]. The energy required for ED could be produced in Reverse Electrodialysis (RED), prior to ED [1]. Reverse electrodialysis is an IEM-based process which harvest energy from a salinity gradient. Seawater is used as a high salinity stream in RED while treated wastewater can be used as a sustainable low salinity stream. However, treated wastewater contains organic micropollutants (OMPs). In a hybrid desalination processes, where RED is used as a pretreatment step for drinking water production, the reuse of treated wastewater is related with a hazard of OMPs contamination of the seawater stream, which ultimately will be the source of drinking water [7].

The term OMPs refers to any organic contaminant of anthropogenic origin (e.g., pesticides, herbicides, personal care products, or pharmaceuticals) at ng L^{-1} up to μg L^{-1} concentration range [8–15]. Several studies have reported the hazard posed by OMPs to the health of humans and animal species. For instance, blocking or disrupting the function of hormones by the endocrine disrupting chemicals occurring in wastewater, and increasing antibiotic resistance of bacteria resulting from the occurrence of pharmaceuticals in the environment [16,17]. Due to the negative impact of OMPs on human health, it is of crucial importance to investigate their interactions with IEMs and their transport in RED systems, where treated wastewater is used as a low salinity stream.

Previous studies found that the sorption of steroidal hormones on IEMs is based on hydrogen bonding and π-cation interactions [18]. Also, diffusion with a strong contribution of convection (caused by electro-osmotic water transport) was observed as responsible for the transport of neutral organic solutes in ED [19,20]. On the other hand, diffusion was recorded as the main transport mechanism responsible for transport of OMPs of various physicochemical properties (i.e. charge, size, and hydrophobicity) in ED, while the convection was neglected [21,22]. In the same studies, it was identified that applied current density has an insignificant effect on the transport rate of OMPs and Donnan dialysis facilitates the transport of charged OMPs under open-circuit conditions.

Varied hypothesis on the transport of OMPs in IEMs originate from the fact that researchers are approaching the same issue from different perspectives and there is a lack of a universal transport model of OMPs in IEMs. Also, the literature on OMPs transport and adsorption in IEMs is very limited; especially, knowledge about behavior of OMPs under open-circuit conditions (RED) is missing. Moreover, research on OMPs' behavior in IEMs has always been investigated either in the field of transport or adsorption only. These two phenomena have never been analyzed together, which makes a consolidated view on OMPs' behavior in IEMs difficult as the type and strength of the bond responsible for the adsorption can either increase or decrease the transport.

The aim of the current research is to establish a connection between adsorption and transport of OMPs in IEMs during the RED process using cross-flow stack in adsorption and zero-current experiments. To mimic the composition of treated wastewater, a mixture of nineteen OMPs of varied physicochemical characteristics (e.g. size, charge, polarity, hydrogen donor/acceptor count, hydrophobicity) at environmentally relevant concentrations was used. A rigorous statistical analysis was conducted to elucidate the main interacting mechanisms between OMPs and IEMs as a function of their physicochemical characteristics, solution chemistry, and experimental conditions. These results highly contribute to: a) providing a rational basis for the optimization/design of next generation IEMs, and b) understanding of the potential hazard posed by OMPs in RED seawater pre-desalination systems, when treated wastewater is used as a low salinity stream. Finally, the current investigation is the first in its field to provide a detailed statistical analysis for correlating the transport behavior of OMPs in RED systems with their physicochemical characteristics; thus, clearly evidencing the importance of surface interactions at the membrane-solution interphase. Also, this study creates a strong link between the extensive knowledge of the performance of ion-exchange membrane processes, interfacial science & technology and organic chemistry.

2. Materials and methods

2.1. Organic micropollutants

Nineteen OMPs were selected based on their environmental relevance and varied physicochemical properties (Supplementary information (SI), Table S1, Table S2). The selection of the physicochemical properties of OMPs used in the data analysis process (Table S1), was based on the different characteristics of the OMPs structure. For instance, a group of properties described the size and shape of the molecules (e.g. Van der Waals radius and solvent accessible surface area) while other group of properties reflected the possibility of occurrence of various non-covalent bonding (e.g. ring count, aromatic ring count, LogP). A 2 mg L^{-1} (each organic solute) stock solution containing an aqueous mixture of all OMPs (analytical grade, Sigma-Aldrich, > 98%) was prepared and stored at 4 °C. The stock solution was diluted to a final concentration of 100 μg L^{-1} (each organic solute) for further experiments.

2.2. Chemical analysis

The concentration of OMPs in solution was analyzed by a liquid chromatography-mass spectrometer (Agilent 6420 LC-MS/MS) with selective electrospray triple quad LC-MS/MS multiple reaction monitoring (MRM) transitions. A Phenomenex phenyl-hexyl column (150 mm × 3 mm, 3 μm pore size) equipped with a guard column was used for separation. The aqueous neutral mobile phase was prepared with 2.5 L milliQ water, 5 mL ammonia 5 M, 1 mL formic acid 99%, and 0.1 mL oxalic acid 1 M. Acetonitrile was used as organic mobile phase B. The samples (1 mL) were spiked with a matrix modifier (50 μL) (to overcome matrix effects), and an internal standard (50 μL). For data analysis, the Agilent Mass Hunter Quant software was used to integrate and quantitate the peaks in the data files.

2.3. Experimental setup

Experiments were conducted in a cross-flow IEM membrane stack (REDstack BV, the Netherlands). The experimental setup flow diagram is shown in SI, Fig. S1. An artificial solution mimicking treated wastewater was prepared with a salinity of 0.017 M (sodium chloride, Sigma-Aldrich) and a 100 μg L^{-1} concentration of OMPs. As artificial seawater, a sodium chloride (Sigma-Aldrich) solution of 0.5 M was used. The stack consisted of five cell pairs of alternating anion- (AEMs) and cation-exchange membranes (CEMs). To create flow compartments between the membranes, custom-made spacers of 270 μm were used (Deukum, Germany). In the electrolyte compartments, silicone gaskets

of 346 µm were used as an additional sealing to prevent any leakage. The membranes at the end of the stack were CEMs (Neosepta CMX), while the inner membranes were Fujifilm type 10 AEMs and CEMs (Fujifilm, the Netherlands). These membranes are commercially used for electrodialysis. The characteristics of these commercial membranes can be found in SI, Table S3. The platinum-coated electrodes on each side of the stack were connected to a potentiostat (A85111, Ivium Technologies, the Netherlands). 5 L amber glass bottles (Schott, Germany) were used as wastewater and seawater containers. Bottles were placed on mass balances (MS8001TS, Mettler Toledo, Germany) to record changes in the mass of wastewater and seawater, from which the water transport was calculated. 5 L of 0.5 M sodium sulfate (Sigma-Aldrich) was used as an electrode rinse solution (ERS). The system components were connected by a 4 mm inner diameter polyethylene tubing. Masterflex L/S peristaltic pumps (Cole-Parmer Instruments, USA) were used for the wastewater, seawater, and ERS channels. An automatic fraction collector (LGS B.V., Ubbena, the Netherlands) was used to collect samples for LC-MS analysis. Three-way magnetic valves (CS3-230 AC) were used in a combination with digital timers (JP Fluid Control, the Netherlands) to collect samples at specified time intervals. After experiments, all reagents and solutions were properly disposed following safety procedures.

2.4. Experimental procedure

2.4.1. Adsorption of OMPs in RED membrane stack

Adsorption experiments were performed to investigate the uptake of OMPs in the RED system, which was not previously exposed to OMPs. Therefore, artificial wastewater (0.017 M NaCl and 100 µg L^{-1} OMPs) was recirculated batch-wise through the system (in all RED compartments) at a flow rate of 170 mL min^{-1} (0.105 m s^{-1}). The adsorption test was conducted in two consecutive experimental steps of 24 h, hereinafter referred to as ES1 and ES2. This time was arbitrarily selected as sufficient time to observe the adsorption. After the first 24 h (ES1), the initial solution was replaced with fresh artificial wastewater at the same initial concentration of OMPs, and the procedure continued for another 24 h (ES2). The sorption of OMPs was calculated as shown in Eq. (1).

$$adorption\ (\%) = \frac{n_0 - n_t}{n_0} \cdot 100\% \quad (1)$$

where, n_0 and n_t are the initial and final amounts of OMPs [moles] for each adsorption step (each after 24 h).

2.4.2. Transport of OMPs under open circuit conditions

To investigate the transport of OMPs driven by the concentration gradient between the wastewater and seawater, open circuit experiments were performed. Artificial wastewater was used as a low salinity stream, while artificial seawater (0.5 M NaCl) was used as a high salinity stream. To investigate the possible effect of flow velocity, the experiment was performed under two flow rates: of 170 mL min^{-1} (flow velocity of 0.105 m s^{-1} and residence time of 0.952 s) and 100 mL min^{-1} (flow velocity of 0.062 m s^{-1} and residence time of 1.62 s). Both experiments were performed for 96 h (i.e. as sufficient time) for observing the transport of OMPs through IEMs based on previous studies, where the diffusion at the same concentration differences was already observed after 48 h [21]. The mass balance over the system at the end of the experiment was calculated for all OMPs individually according to Eqs. (2) and (3):

$$transport = \left(\frac{n_{SW}(t)}{n_{IW}(t=0)} \cdot 100\% \right) \quad (2)$$

$$adsorption = \left(1 - \left(\frac{n_{IW}(t) + n_{SW}(t)}{n_{IW}(t=0)} \right) \right) \cdot 100\% \quad (3)$$

where, $n_{IW}(t = 0)$ is the initial amount of OMP [moles] in impaired water, which is the total amount of OMP in the system in the experimental phase. $n_{IW}(t)$ and $n_{SW}(t)$ are the amounts of OMP [moles] in impaired water and in seawater, respectively, after 96 h.

2.5. Statistical analysis

A principle component analysis (PCA) was used to reduce the number of dimensions of the data set and physicochemical properties of the compounds. PCA displays objects in a reduced space by finding directions (principal components) that best preserve the scatter of the observations (values) in the multidimensional space, thus, resulting in orthogonal (uncorrelated) factors. PCA analyzes total (common and unique) variance.

A Pearson correlation matrix was used to investigate the influence of each of the physicochemical characteristics of the OMPs on the adsorption and transport. Calculation details are included in SI, Appendix A.

3. Results and discussion

3.1. Adsorption of OMPs in RED stack

The membrane stack used in this study consisted of five AEMs and six CEMs. The adsorption of positively charged OMPs was the highest (50–100%) among investigated compounds in both experimental steps (ES1 and ES2), except for pirimicarb (Fig. 1). On the contrary, negatively charged OMPs showed low adsorption (up to 10%) in the ES1, except for diclofenac (Fig. 1), while in the ES2, adsorption was minor. Interestingly, triclopyr and ibuprofen desorbed from membranes in the ES2 (Fig. S2, SI). The exceptional behavior of pirimicarb and diclofenac will be explained further in this section. Correspondingly to negatively charged, non-charged OMPs were also characterized by low adsorption in the ES1 and desorption of two compounds (i.e., caffeine and dimethoate) in the ES2 (Fig. S2, SI). Based on these observations and the analysis of concentration profiles (Fig. S2, SI), it was concluded that the mechanism of the OMPs adsorption in the IEMs is dependent on their charge. Thus, electrostatic interactions (i.e. long-range forces) govern the adsorption of OMPs in the RED system in the first place.

For a better understanding of the adsorption mechanisms of OMPs, a Pearson correlation matrix between calculated adsorption and the physicochemical parameters of OMPs (Table S1, SI) was determined (Fig. 2). This correlation was conducted separately for positively,

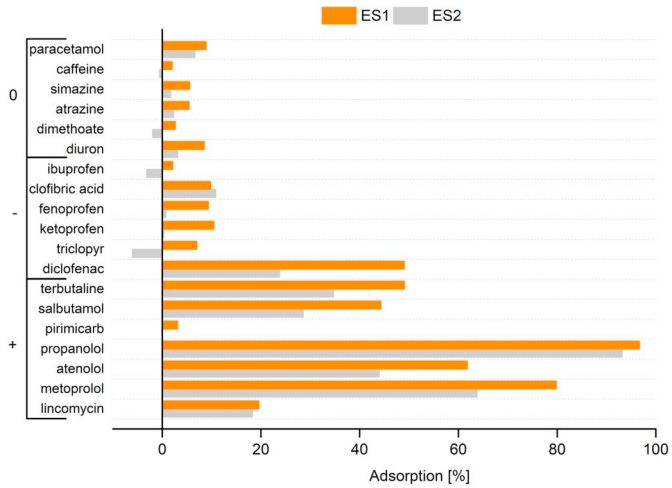

Fig. 1. Adsorption of organic micropollutants (OMP) in ion-exchange membrane stack. OMPs are ordered by charge. Artificial wastewater (0.017 M NaCl with 100 µg L^{-1} each OMPs) was pumped batch-wise through the system. After the first 24 h (ES1), the solution was replaced with fresh artificial wastewater (ES2). The procedure continued for another 24 h.

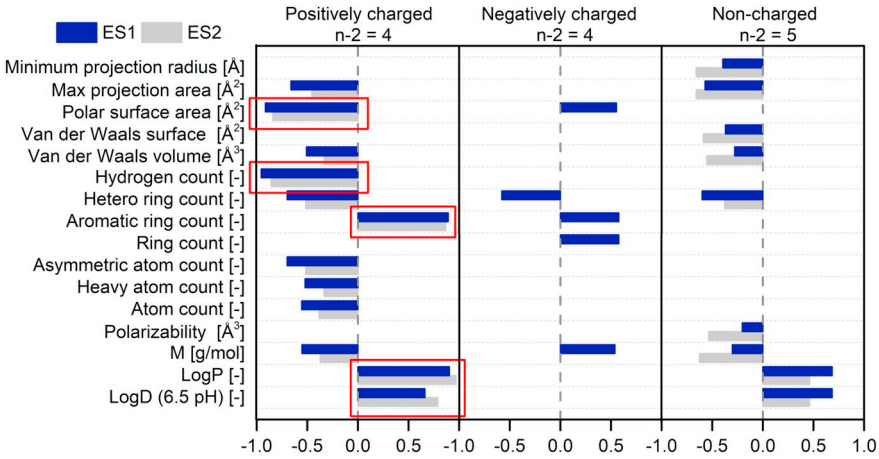

Fig. 2. Pearson correlation coefficients (r) between adsorption and physicochemical parameters of positively-charged, negatively-charged, and non-charged compounds, with n-2 degrees of freedom. Only those correlations where at least one experimental step (i.e. ES1 or ES2) was characterized by a strong correlation coefficient ($r \geq 0.5$ or $r \leq -0.5$) were shown on the plot. The correlations where p-value was lower than the level of significance ($\alpha = 0.05$) are indicated by the red frames. (For interpretation of the references to color in this figure legend, the reader is referred to the web version of this article.)

negatively, and non-charged OMPs. Multiple strong correlations between adsorption and physicochemical parameters were observed (e.g. correlation between polar surface area and adsorbed amount of positively charged OMPs). However, only the correlations for partition coefficient (LogP), distribution coefficient (LogD), aromatic ring count, hydrogen donor/acceptor sum count, and polar surface area for positively-charged OMPs were characterized by p-values lower than the level of significance ($\alpha = 0.05$). From a statistical point of view, these results would indicate the rejection of the null hypothesis for the rest of the correlations where p-value were higher than the level of significance ($\alpha = 0.05$). Nevertheless, the use of statistical significance as a tool to validate or reject the correlation between adsorption and selected parameters (i.e. physicochemical characteristics) cannot be fully justified due to the specific experimental conditions in the current study. Specifically, the number of tested compounds in each group (i.e. positively-, negatively-, and non-charged) is small; thus, leading to: i) a low value of degrees of freedom, and ii) a statistic impact on the obtained p-values. The experimental design fulfilling statistical requirements (i.e. expanding the number of OMPs) is a complex task, due to limits of analytical techniques and possible chemical interactions between OMPs. Although the Pearson correlation analysis approach suffers from the mentioned limitations, the hypothesis presented in this investigation are highly consistent and supported by previous literature.

The adsorption of positively charged OMPs was characterized by a strong, positive correlation with the aromatic ring count (Fig. 2). It is concluded that the more aromatic rings are present in the structure of OMPs, the higher quantity of the OMPs adsorbs. This indicates the importance of π-π interactions formed by electrons in overlapping parallel p orbitals between the aromatic ring in OMPs and IEMs [23]. π-π interactions have been reported as the leading mechanism facilitating the adsorption of pharmaceuticals on carbon-based adsorbents [24]. Similar to this previous study, π-π interactions played a key role in the current investigation. However, based on observed correlations in this study, π-π interactions cannot be stated as the leading mechanism.

LogP and LogD were also positively correlated with the adsorption, indicating an important role of hydrophobic interactions in the OMPs adsorption on IEMs. The importance of these interactions is also supported with a negative correlation between total hydrogen donor/acceptor count and the adsorption. Specifically, the presence of hydrogen donor/acceptor counts in the molecule increases its hydrophilicity. The identified correlations in this study emphasize the importance of hydrophobic interactions for the adsorption of the selected positively charged OMPs. Thus, it shows that the effect of hydrophobic interactions is more important for the adsorption than the effect of hydrogen bonding in the selected group of compounds.

Hydrophobic interactions depend on the size and shape of the hydrophobes [25,26], indicating that steric hindrance is a limiting factor for the adsorption induced by hydrophobic interactions. Size and shape, represented by topological polar surface area (strong correlation, supported by p-value) and molecular mass, heavy atom count, Van der Waals volume, and minimum projection area showed a negative correlation with the adsorption. For example, the effect of steric hindrance on the adsorption is particularly influential for lincomycin, which is characterized by the largest molecular size; thus, its adsorption was very low (< 20%).

Pirimicarb was an exception among positively charged OMPs characterized by the lowest adsorption (< 5%) (Fig. S2, SI). Contrary to other positive OMPs, pirimicarb is characterized by a significantly lower charge (formal charge of 0.24 [−]), while those of the others were approximately one (Table S1, SI). Therefore, due to a lower influence of its charge, pirimicarb behaved similarly to a non-charged OMPs.

The system capacity to adsorb negatively charged OMPs was lower comparing to positively charged OMPs. Saturation was already achieved in ES1 (Fig. 1); thus, only ES1 was considered in the correlation analysis. The adsorption of negatively charged OMPs was correlated with aromatic ring count, indicating the importance of π-π interactions. This is also in line with previous observations reporting the adsorption of diclofenac to graphene oxide [27].

Diclofenac was characterized by the highest adsorption among negatively charged OMPs, which was related to molecular volume and hydrophobicity. Diclofenac has the largest molecular volume compared to other negatively charged OMPs. Therefore, the possibility of interaction between diclofenac molecules and adsorbent is the largest, leading to higher adsorption. Hydrophobicity, which can be described by the LogP and LogD, played a crucial role in the adsorption of diclofenac. Both LogP and LogD refer to the ratio of the concentration of the compound between the aqueous and octanol phase. However, LogP only includes neutral species, while LogD includes both charged and uncharged species [28]. Diclofenac has the highest LogP value (4.26), while its LogD is moderate (1.79) among other OMPs used in this study. This suggests that adsorption mechanism of diclofenac is based on physical affinity on its neutral, non-dissociated form. This finding remains in agreement with previous results reporting that lipophilicity is necessary to drive the solutes to the interfacial region of a membrane [29].

Oppositely to positively charged OMPs, the adsorption of negatively charged OMPs followed the Traube's rule, which explains the effect of the chain length and molecular size on the adsorption [30]. Specifically, in a situation where the affinity between solute and adsorbent is low, a larger size of the solute creates a larger contactable surface area between the solute and the adsorbent (membrane), and thus a higher likelihood to effectively interact with the membrane. This indicates that negatively charged OMPs are adsorbed at the surfaces of the membranes, while positively charged OMPs are adsorbed inside the

membranes.

Adsorption of non-charged OMPs is not influenced by electrostatic interactions, thus it is based on short-range interactions occurring at the interface of the membranes. Hydrophobic interactions are expected to be the most influential type of interactions responsible for the adsorption of non-charged OMPs. This is because of a positive correlation between LogP and the adsorption. Negative correlations between adsorption and size/shape parameters were observed; thus, indicating the importance of effect of the steric hinderance in the same way as it was observed for positively charged OMPs. Thus, it can be also concluded that adsorption of non-charged OMPs occurs inside the membrane polymer.

3.2. Open circuit experiment

The transport of OMPs in RED stack was investigated under a chemical potential gradient from feed (artificial wastewater) to artificial seawater. The effect of flow velocity in the stack was also studied, for which the experiment was conducted under two different flow rate conditions: 100 and 170 mL min^{-1}, resulting in flow velocities of 0.105 and 0.062 m s^{-1}, respectively.

Fig. 3 shows the transport and adsorption of OMPs in the system (calculated according to Eq. (2) and Eq. (3)). Pirimicarb, atrazine, simazine, and caffeine exceeded the mass balance, due to desorption on the feed side. The transport of positively charged OMPs was below 10%, while its adsorption was still significant. Negatively charged compounds showed the highest transport. Non-charged compounds were

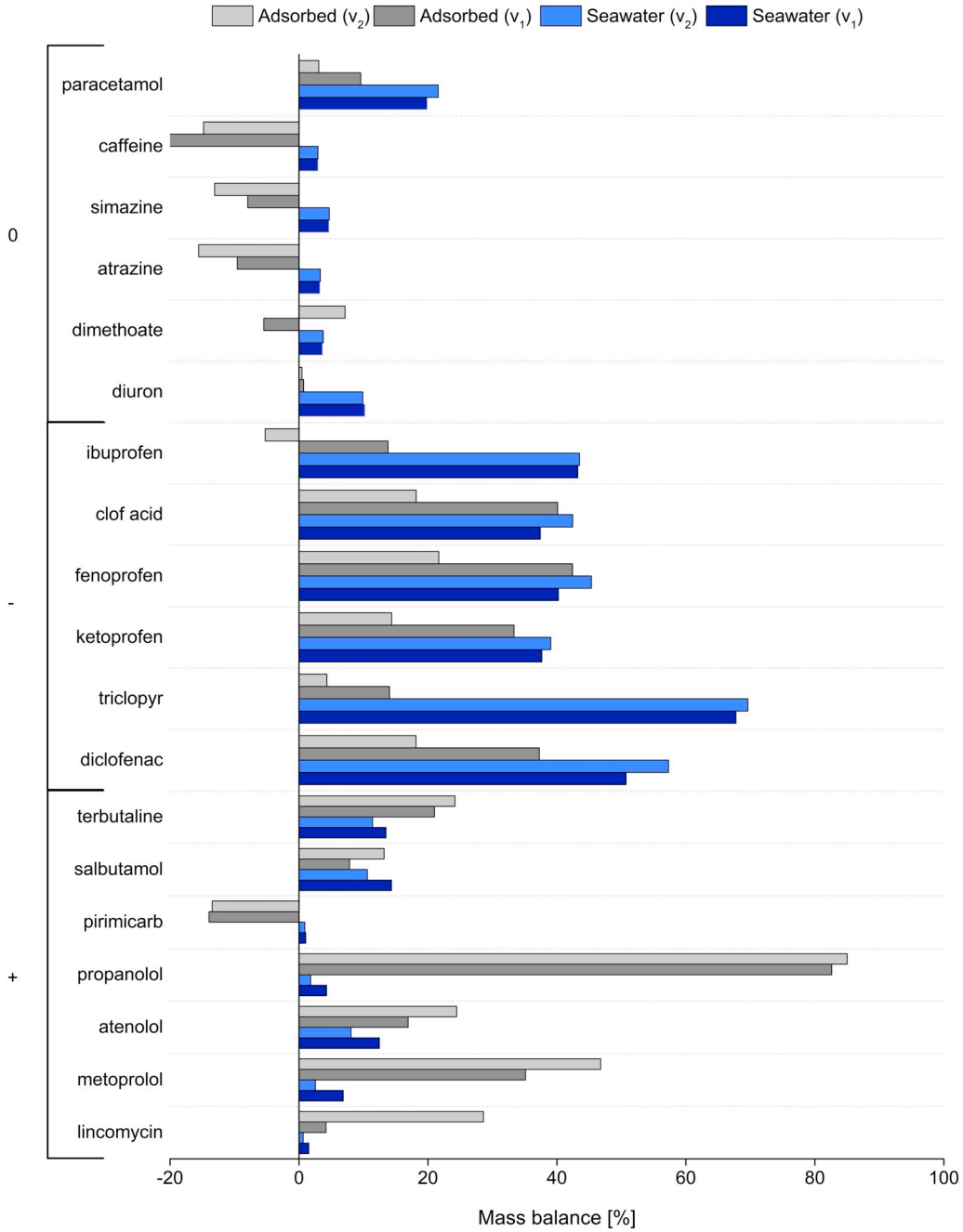

Fig. 3. Transport toward seawater compartment and adsorption of organic micropollutants (OMP) in the system for zero current experiments, where $v_1 = 0.105$ m s^{-1} and $v_2 = 0.062$ m s^{-1}. Artificial wastewater (0.017 M NaCl with 100 μg L^{-1} of each OMPs) was used as concentrate, while an artificial seawater (0.5 M NaCl) was used as a diluate. Experiments were conducted in a batch-wise mode for 96 h, for two flow velocities: 0.105 and 0.062 m s^{-1}.

hardly adsorbed.

Under both flow velocities, the adsorption of negatively charged OMPs was higher compared to ES1 and ES2 described in Section 3.1. In ES1, the adsorption of negatively charged OMPs was approximately 15%, while in ES2 it hardly occurred (Fig. 1). Under open circuit conditions, only ibuprofen and triclopyr still showed low adsorption (approx. 15%). Clofibric acid, fenoprofen, ketoprofen, and diclofenac were highly adsorbed, i.e. approx. 40% at a flow velocity of 0.105 m s^{-1}, and approx. 20% at a flow velocity of 0.062 m s^{-1}. The different behavior of ibuprofen and triclopyr is consistent with results explored in Section 3.1. Specifically, larger negatively charged compounds are more favorably adsorbed onto the IEMs. Ibuprofen is the compound characterized by the lowest molecular mass, and triclopyr has the lowest Van der Waals volume. Based on the differences between the adsorption and open circuit experiments, the later one has a higher driving force to transport organic molecules to the membrane phase. This is because the concentration gradient is established not only between the surrounding solution and membranes, but across the membranes (the difference in OMPs concentration between wastewater and seawater). An increased adsorption was observed only for negatively charged OMPs among positively and non-charged OMPs in open circuit experiments. In the Section 3.1, it was found that negatively

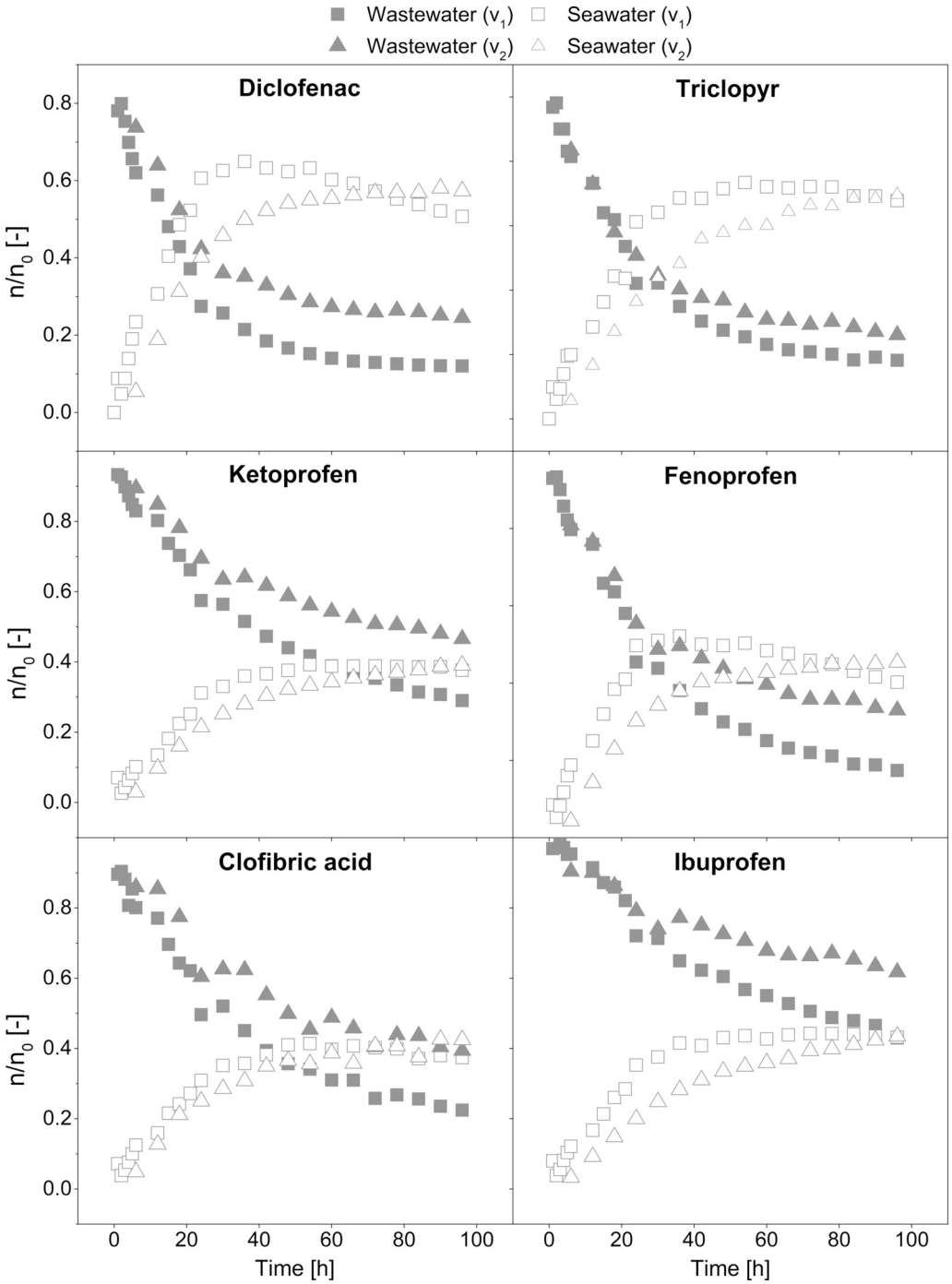

Fig. 4. Concentration profiles of negatively charged OMPs during RED experiment in wastewater (feed) and in a seawater compartment, where v_1 = 0.105 m s^{-1} and v_2 = 0.062 m s^{-1}. Profiles are shown for two experiments of 0.105 (squares) and 0.062 (triangles) ms^{-1} flow velocity. Part of the compounds exceeded the concentration level in seawater corresponding to the diffusion equilibrium, and transport occurred against their concentration gradient.

charged OMPs are adsorbed at the surface of the membranes, while positively and non-charged OMPs adsorbed inside the membranes. In open circuit experiments, however, due to higher driving force, which overcomes the surface energy barrier and drags the negatively charged OMPs to the seawater, negatively charged OMPs penetrate membrane structure and adsorb inside the membrane phase.

Furthermore, most of the negatively charged OMPs exceeded the concentration level in artificial seawater stream corresponding to the diffusion equilibrium (Fig. 4). After reaching equimolar concentration in seawater and wastewater, the transport of negatively charged OMPs continued against the concentration gradient. Since open circuit experiments were performed without the net flux of electrical charges, this phenomenon is explained by an uphill transport caused by Donnan dialysis. When two types of chemical potentials carry the same type of charge (e.g., chloride and negatively charged OMPs) and these potentials are oriented in a counter-direction, the system tends to a thermodynamic equilibrium [31]. Since $\Delta E_{Cl^-}{}^0 > > \Delta E_{OMP^-}{}^0$, the difference between those potentials is a driving force for the uphill transport of OMPs, driven by the downhill transport of Cl^-, as OMPs are weak electrolytes and are present at a significantly lower concentration than NaCl. Fig. 4 also shows the effect of the flow velocity of diluate and concentrate streams on the transport of negatively charged OMPs through the IEMs. The concentration profiles are steeper at the higher flow velocity. Thus, the transport does not depend on the retention time of a single pass of solution, but on the total number of passes of the solution through the membrane stack. The concentration profiles shown in Fig. 4 are not symmetric due to the adsorption.

Positively charged OMPs were not transported through the IEMs with Donnan dialysis, despite that the same driving force, as for negatively charged OMPs, also applies to them. Positively charged OMPs interact with membranes through strong electrostatic, hydrophobic, and π-π interactions (Section 3.1). Although those are non-covalent interactions, they induce a strong adsorption, which hinders the transport of OMPs. On the other hand, it can be expected that charged OMPs follow Donnan exclusion effect and thus, positively charged OMPs are mainly transported through the CEMs, while negatively charged OMPs are mainly transported through AEMs. Even if the membranes are the same type, AEMs and CEMs vary in their structural properties, such as e.g. polymer density or membrane crosslinking. The charge density and thus, the number of active sites for charge-based adsorption also varies between AEMs and CEMs. This results in a difference in the adsorption and transport properties toward OMPs. For instance, higher crosslinking of the membrane polymer in CEMs increases their surface energy barrier and thus the impact of the steric hindrance for the transport of positively charged OMPs. Also, a higher polymer density results in higher number of adsorption active sites and higher adsorption capacity toward positively charged OMPs. A very high adsorption capacity of CEMs toward positively charged OMPs could explain the low transport. Membranes did not reach saturation, therefore, all compounds which entered the membranes were adsorbed inside. The adsorption bonding would be much higher than Donnan potential.

To investigate the effect of the adsorption on the transport through the RED stack, a Pearson correlation was performed between the adsorption from ES1 and ES2 (Section 3.1, Fig. 1), the adsorption from open circuit experiments, and the transport observed in open circuit experiments (Fig. 3). Based on this analysis, only the transport of non-charged OMPs showed a strong (positive) correlation with adsorption in both experiments (Fig. 5). It should be noted that these results are statistically relevant, as calculated p-values are lower than the level of significance ($\alpha = 0.05$). As aforementioned, the transport of non-charged OMPs inside the IEMs is driven by the diffusion. According to solution-diffusion model, adsorption is the first step of the transmembrane transport, occurring at the membrane surface. Thus, easy adsorption at the membrane surface accelerates the transport. Therefore, the measured adsorption is coupled with the transport. Because it is observed for the non-charged OMPs only, it can be concluded that solution-diffusion model is a valid transport model describing transport of non-charged OMPs through IEMs.

For a better understanding of the transport phenomena of OMPs in IEMs, a correlation analysis with different molecular properties was performed. The Pearson correlation coefficients matrix between the measured transport (% in Seawater) and the physicochemical parameters of the compounds was determined. This correlation was performed separately for positively, negatively, and non-charged OMPs. Fig. 6 summarizes correlations, characterized by strong correlation coefficients (i.e. $r \geq 0.5$ and $r \leq -0.5$).

Multiple strong correlations between transport and physicochemical parameters of positively-charged, negatively-charged, and non-charged OMPs were observed. However, similar to the adsorption experiments (Section 3.1), only correlations for positively charged compounds were characterized by p-values lower than the level of significance ($\alpha = 0.05$).

Positively charged compounds did not show a positive correlation with any of the investigated parameters. The importance of the steric hindrance was indicated by a strong negative correlation between transport and parameters representing the conformation (size and shape) of the molecule (e.g., maximum projection area). For instance, lincomycin is the largest compound of the group and was hardly transported (Fig. 3) due to steric hindrance. The steric effect has been widely reported as a factor affecting the rejection of organic solutes in pressure driven membranes in accordance with IEMs [32–35].

Strong, positive correlations between transport, topological polar surface area and hydrogen count were found for negatively charged OMPs (Fig. 6). Topological polar surface area is defined as the area of its Van der Waals surface arising from oxygen or nitrogen atoms or hydrogen atoms attached to oxygen or nitrogen atoms. As such, it is a measure of the compound capacity to form hydrogen bonds [36]. The

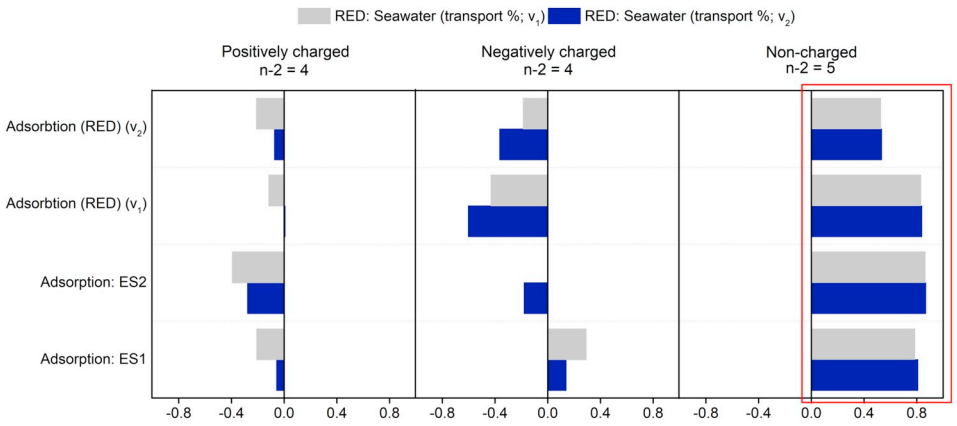

Fig. 5. Correlation analysis between the adsorption (%) from the adsorption experiment (ES1 and ES2, Section 3.1) and the adsorption (%) and transport (%) from the RED experiment. RED experiment was operated in two flow velocities of feed (artificial wastewater) and diluate (artificial seawater), where $v_1 = 0.105\,m\,s^{-1}$ and $v_2 = 0.062\,m\,s^{-1}$. Only non-charged OMPs showed a strong correlation with adsorption in both experiments ($r \geq 0.5$ or $r \leq -0.5$), confirmed by p-values lower than the level of significance ($\alpha = 0.05$) (indicated by red frames). (For interpretation of the references to color in this figure legend, the reader is referred to the web version of this article.)

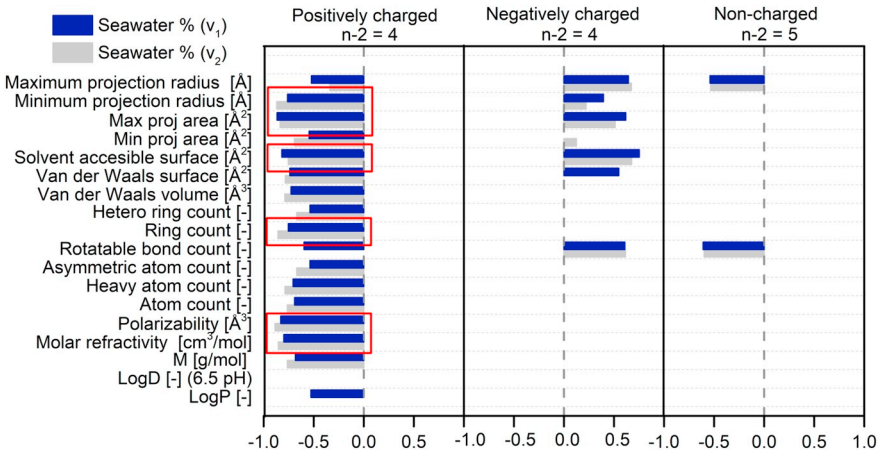

Fig. 6. Pearson correlation coefficients (r) between transport (% in Seawater) and physicochemical parameters of positively-charged, negatively-charged, and non-charged compounds, with n-2 degrees of freedom. RED experiment was operated in two flow velocities of feed (artificial wastewater) and diluate (artificial seawater), where $v_1 = 0.105\,m\,s^{-1}$ and $v_2 = 0.062\,m\,s^{-1}$. Only correlations characterized by a strong correlation coefficient: $r \geq 0.5$ and $r \leq -0.5$ were shown on the plot. The correlations where p-value ≤ than the level of significance ($\alpha = 0.05$) are indicated by red frames. (For interpretation of the references to color in this figure legend, the reader is referred to the web version of this article.)

effect of topological polar surface area is in line with the hydrogen sum count. The strong positive correlation with the hydrogen count suggests hydrophilicity as a mechanism transporting the molecule out of the membrane. Strong correlation between transport and hetero ring count was also found (Fig. 6). This observation is consistent with the findings from the adsorption experiment (Section 3.1), where hetero ring count was negatively correlated with the adsorption of all OMPs, representing that a lower affinity to the membrane phase improves its desorption from the membrane after crossing it.

The correlation analysis of non-charged OMPs showed that their transport is dependent on steric hindrance. The transport of non-charged OMPs is diffusion driven and governed by their chemical potential difference. Due to the lack of charge, non-charged OMPs do not undergo Donnan exclusion, and thus can be transported through both CEMs and AEMs. Because of the low driving force, i.e. low concentration of organic solutes in experiment, the transport was not significant.

3.3. PCA and general discussion

PCA was performed to further validate the relation between the properties of the compounds and their influence on adsorption and transport of OMPs. This analysis was performed: a) on the physicochemical properties, and b) on the measured adsorption (ES1 and ES2), measured transport in open circuit experiments, calculated adsorption in open circuit experiments, and measured retention (nor adsorbed or transported amount of OMPs) in open circuit experiment.

Fig. 7 shows that the physicochemical properties are grouped into three clusters. In the first cluster; LogP, ring count, and aromatic ring count were the most important properties for the determination of the physical meaning of component 2. Also, these three properties were the second most important parameters determining adsorption. The second and the largest group comprised the properties responsible for the conformation of OMPs. The third group contained hetero ring count, hydrogen donor/acceptor count, topological polar surface area, and charge properties.

Fig. 8 shows the PCA of the experimental results from both: adsorption (ES1 and ES2) and RED, i.e. adsorption, transport (seawater) and retention (wastewater). PCA confirmed charge as the most influential solute parameter governing adsorption and transport of OMPs. Positively charged compounds were clustered near the adsorption, negatively charged compounds were grouped near the transport, while non-charged compounds were grouped near the retention (wastewater) due to their low permeability and low adsorption. The analysis of the location of the vectors representing experimental results showed that

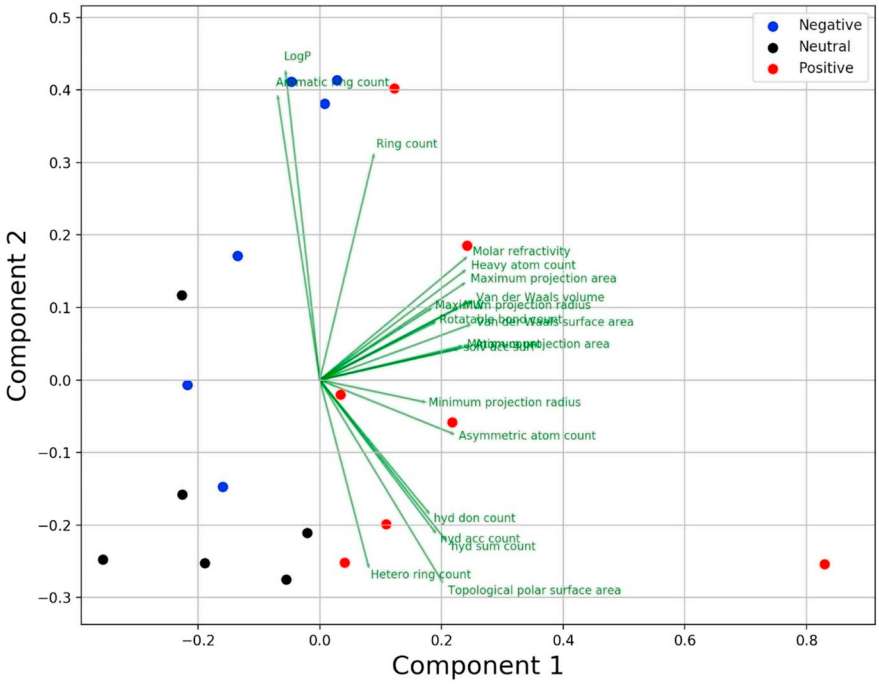

Fig. 7. PCA of physicochemical properties of OMPs displayed the results in the orthogonal dataspace, where green vectors indicate the physicochemical properties of compounds, while points represent the position of certain compounds versus principal component 1 and principal component 2. (For interpretation of the references to color in this figure legend, the reader is referred to the web version of this article.)

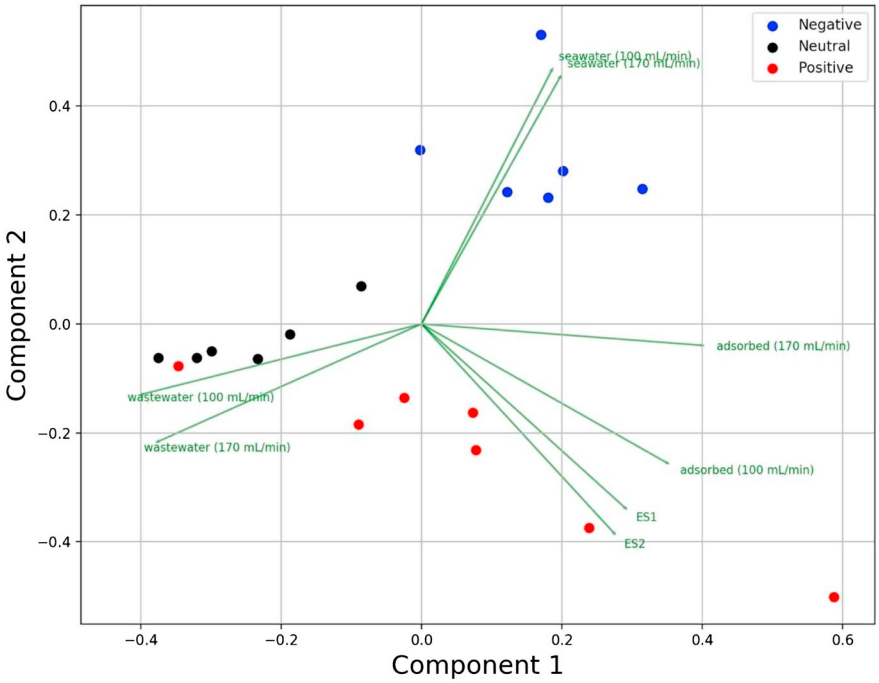

Fig. 8. PCA of experimental results from: adsorption (ES1 and ES2) and open circuit experiments, i.e. adsorption, transport (seawater) and retention (wastewater). Results are displayed in the orthogonal dataspace, where green vectors indicate the experimental results, while points represent the position of certain compound versus principal component 1 and principal component 2. (For interpretation of the references to color in this figure legend, the reader is referred to the web version of this article.)

adsorption results are grouped, independently from the experiments. Also, PCA results confirmed that positively charged OMPs are mainly adsorbed, negatively charged OMPs are mainly transported, while non-charged compounds are mainly retained in the feed solution.

4. Conclusions

This research identified the types of molecular interactions determining the adsorption and transport properties of OMPs in IEMs. In this study we presented that the charge (long-range forces) of the OMPs primarily governs their adsorption and transport in IEMs stack, and another non-covalent interactions secondarily determine the behavior of OMPs at the surface of membranes.

Positively charged OMPs were characterized by the highest adsorption (50–100%), where π-π interactions and hydrophobic interactions were found to be the secondary-forces responsible for the adsorption that occurred inside the membrane. Under open circuit conditions, positively charged OMPs were highly adsorbed and were not significantly transported (below 20%), even though they undergo Donnan dialysis driving force. Large capacity of CEMs to adsorb the positively charged OMPs and strength of the adsorption bonding overcame the effect of the Donnan potential.

Negatively charged OMPs were adsorbed in a significantly lower amount compared to positively charged OMPs (10–20%). In ES1 and ES2 adsorption occurred at the surface of AEMs, due to hydrophobic interactions. In open circuit experiments, negatively charged OMPs were transported across the membraned due to Donnan dialysis. Also, in this experiment adsorption increased and occurred inside the membranes, as the Donnan potential overcame the surface energy barrier of AEMs.

Non-charged OMPs were hardly adsorbed in every experiment (below 10%) and the adsorption mainly occurred due to hydrophobic and π-π interactions inside the membrane polymer. In open circuit experiments, non-charged OMPs were transported by diffusion. Diffusional transport of non-charged OMPs was coupled with adsorption, which confirmed the validity of the solution-diffusion model in the description of their transport in IEMs.

Acknowledgments

This work was performed in the cooperation framework of Wetsus, European Centre of Excellence for Sustainable Water Technology (www.wetsus.eu). Wetsus is co-funded by the Dutch Ministry of Economic Affairs and Ministry of Infrastructure and Environment, the Province of Fryslân, and the Northern Netherlands Provinces. This project has also received funding from the European Union's Horizon 2020 research under grant agreement No 685579 (www.revivedwater.eu). The authors would like to thank the participants of the research theme “Blue Energy” for their input, suggestions and their financial support. Finally, the authors would like to express their gratitude to the Wetsus technical support team.

Appendix A. Supplementary data

Supplementary data to this article can be found online at https://doi.org/10.1016/j.desal.2019.114084.

References

[1] M. Vanoppen, G. Blandin, S. Derese, P. Le Clech, J. Post, A.R.D. Verliefde, Salinity gradient power and desalination, Salinity Gradient Power and Desalination. Sustainable Energy From Salinity Gradients, Woodhead publishing, London, 2016.
[2] A. Galama, M. Saakes, H. Bruning, H. Rijnaarts, J. Post, Seawater predesalination with electrodialysis, Desalination 342 (2014) 61–69.
[3] M. Elimelech, W.A. Phillip, The future of seawater desalination: energy, technology, and the environment, science 333 (2011) 712–717.
[4] M. Vanoppen, Ion-Exchange Based Processes in Hybrid Water Treatment, Ghent University, 2016.
[5] B. Van der Bruggen, C. Vandecasteele, Distillation vs. membrane filtration: overview of process evolutions in seawater desalination, Desalination 143 (2002) 207–218.
[6] V.G. Gude, N. Nirmalakhandan, S. Deng, Renewable and sustainable approaches for desalination, Renew. Sust. Energ. Rev. 14 (2010) 2641–2654.
[7] M. Vanoppen, E. Criel, G. Walpot, D.A. Vermaas, A. Verliefde, Assisted reverse electrodialysis—principles, mechanisms, and potential, npj Clean Water 1 (2018) 9.
[8] S. Jobling, M. Nolan, C.R. Tyler, G. Brighty, J.P. Sumpter, Widespread sexual disruption in wild fish, Environmental science & technology 32 (1998) 2498–2506.
[9] A.R.D. Verliefde, Rejection of Organic Micropollutants by High Pressure Membranes (NF/RO), Delft University of Technology, TU Delft, 2008.
[10] J.Y. Tang, S. McCarty, E. Glenn, P.A. Neale, M.S.J. Warne, B.I. Escher, Mixture effects of organic micropollutants present in water: towards the development of effect-based water quality trigger values for baseline toxicity, Water Res. 47 (2013) 3300–3314.

[11] Q. Sui, X. Cao, S. Lu, W. Zhao, Z. Qiu, G. Yu, Occurrence, sources and fate of pharmaceuticals and personal care products in the groundwater: a review, Emerging Contaminants 1 (2015) 14–24.
[12] A.J. Ebele, M.A.-E. Abdallah, S. Harrad, Pharmaceuticals and personal care products (PPCPs) in the freshwater aquatic environment, Emerging Contaminants 3 (2017) 1–16.
[13] S. Weigel, J. Kuhlmann, H. Hühnerfuss, Drugs and personal care products as ubiquitous pollutants: occurrence and distribution of clofibric acid, caffeine and DEET in the North Sea, Sci. Total Environ. 295 (2002) 131–141.
[14] A. Ccanccapa, A. Masiá, A. Navarro-Ortega, Y. Picó, D. Barceló, Pesticides in the Ebro River basin: occurrence and risk assessment, Environ. Pollut. 211 (2016) 414–424.
[15] C. Postigo, M.J.L. de Alda, D. Barceló, A. Ginebreda, T. Garrido, J. Fraile, Analysis and occurrence of selected medium to highly polar pesticides in groundwater of Catalonia (NE Spain): an approach based on on-line solid phase extraction–liquid chromatography–electrospray-tandem mass spectrometry detection, J. Hydrol. 383 (2010) 83–92.
[16] N. Bolong, A. Ismail, M.R. Salim, T. Matsuura, A review of the effects of emerging contaminants in wastewater and options for their removal, Desalination 239 (2009) 229–246.
[17] O.A. Jones, N. Voulvoulis, J.N. Lester, Potential impact of pharmaceuticals on environmental health, Bull. World Health Organ. 81 (2003) 768–769.
[18] L.J. Banasiak, A.I. Schäfer, Sorption of steroidal hormones by electrodialysis membranes, J. Membr. Sci. 365 (2010) 198–205.
[19] L. Han, S. Galier, H. Roux-de Balmann, Transfer of neutral organic solutes during desalination by electrodialysis: influence of the salt composition, J. Membr. Sci. 511 (2016) 207–218.
[20] F. Borges, H. Roux-de Balmann, R. Guardani, Investigation of the mass transfer processes during the desalination of water containing phenol and sodium chloride by electrodialysis, J. Membr. Sci. 325 (2008) 130–138.
[21] M. Vanoppen, A.F. Bakelants, D. Gaublomme, K.V. Schoutteten, J.V. Bussche, L. Vanhaecke, A.R. Verliefde, Properties governing the transport of trace organic contaminants through ion-exchange membranes, Environmental science & technology 49 (2014) 489–497.
[22] M. Vanoppen, G. Stoffels, L. Ma, E. De Meyer, K.V. Schoutteten, J.V. Bussche, L. Vanhaecke, A.R. Verliefde, Selective separation of organics and inorganics with ion-exchange membranes: influence of solution matrix and organics properties, Meeting Abstracts, The Electrochemical Society, 2016, p. 1764.
[23] J.F. Bunnett, Organic chemistry: a short course, 10th edition (Hart, Harold; Craine, Leslie E.; Hart, David J.), J. Chem. Educ. 76 (1999) 1341.
[24] B. Peng, L. Chen, C. Que, K. Yang, F. Deng, X. Deng, G. Shi, G. Xu, M. Wu, Adsorption of antibiotics on graphene and biochar in aqueous solutions induced by π-π interactions, Sci. Rep. 6 (2016) 31920.
[25] P.W. Snyder, J. Mecinović, D.T. Moustakas, S.W. Thomas, M. Harder, E.T. Mack, M.R. Lockett, A. Héroux, W. Sherman, G.M. Whitesides, Mechanism of the hydrophobic effect in the biomolecular recognition of arylsulfonamides by carbonic anhydrase, Proc. Natl. Acad. Sci. 108 (2011) 17889–17894.
[26] A.Y. Ben-Naim, Hydrophobic Interactions, Springer Science & Business Media, 2012.
[27] S.-W. Nam, C. Jung, H. Li, M. Yu, J.R. Flora, L.K. Boateng, N. Her, K.-D. Zoh, Y. Yoon, Adsorption characteristics of diclofenac and sulfamethoxazole to graphene oxide in aqueous solution, Chemosphere 136 (2015) 20–26.
[28] L. Xing, R.C. Glen, Novel methods for the prediction of logP, p K a, and logD, J. Chem. Inf. Comput. Sci. 42 (2002) 796–805.
[29] P. Stenberg, K. Luthman, P. Artursson, Prediction of membrane permeability to peptides from calculated dynamic molecular surface properties, Pharm. Res. 16 (1999) 205–212.
[30] G. Barnes, I. Gentle, Interfacial Science: An Introduction, Oxford university press, 2011.
[31] J.W. Post, H.V. Hamelers, C.J. Buisman, Influence of multivalent ions on power production from mixing salt and fresh water with a reverse electrodialysis system, J. Membr. Sci. 330 (2009) 65–72.
[32] B. Van der Bruggen, C. Vandecasteele, Modelling of the retention of uncharged molecules with nanofiltration, Water Res. 36 (2002) 1360–1368.
[33] B. Van der Bruggen, J. Schaep, D. Wilms, C. Vandecasteele, Influence of molecular size, polarity and charge on the retention of organic molecules by nanofiltration, J. Membr. Sci. 156 (1999) 29–41.
[34] Y. Yoon, G. Amy, J. Cho, N. Her, J. Pellegrino, Transport of perchlorate (ClO_4^-) through NF and UF membranes, Desalination 147 (2002) 11–17.
[35] J. Yoon, G. Amy, Y. Yoon, P. Brandhuber, J. Pellegrino, Rejection of target anions; hexavalent chromium (CrO_4^{2-}), perchlorate (ClO_4^-), and arsenate ($H_2AsO_4^-$/$HAsO_4^{2-}$); by negatively charged membranes, Membrane Technology Conference Proceedings, 2003.
[36] D.E. Clark, Rapid calculation of polar molecular surface area and its application to the prediction of transport phenomena. 1. Prediction of intestinal absorption, J. Pharm. Sci. 88 (1999) 807–814.